Toxicology Reports 3 (2016) 295–305

Contents lists available at ScienceDirect

Toxicology Reports

journal homepage: www.elsevier.com/locate/toxrep

Interaction of *p*-benzoquinone with hemoglobin in smoker's blood causes alteration of structure and loss of oxygen binding capacity

Arunava Ghosh[a], Santanu Banerjee[a], Amrita Mitra[b], Monita Muralidharan[b], Bappaditya Roy[a], Rajat Banerjee[a], Amit Kumar Mandal[b], Indu B. Chatterjee[a,*]

[a] *Department of Biotechnology and Dr. B. C. Guha Centre for Genetic Engineering & Biotechnology, University College of Science, Kolkata 700019, India*
[b] *Clinical Proteomics Unit, Division of Molecular Medicine, St. John's Research Institute, 100 ft Road, Koramangala, Bangalore 560034, India*

ARTICLE INFO

Article history:
Received 2 February 2016
Accepted 5 February 2016
Available online 9 February 2016

Keywords:
p-Benzoquinone
Human smoker's hemoglobin
Mass spectrometry
Atomic force microscopy
Oxygen binding capacity
CORM-3
[tricarbonylchloro(glycinato)ruthenium(II)]

ABSTRACT

Cigarette smoke (CS) is an important source of morbidity and early mortality worldwide. Besides causing various life-threatening diseases, CS is also known to cause hypoxia. Chronic hypoxia would induce early aging and premature death. Continuation of smoking during pregnancy is a known risk for the unborn child. Although carbon monoxide (CO) is considered to be a cause of hypoxia, the effect of other component(s) of CS on hypoxia is not known. Here we show by immunoblots and mass spectra analyses that in smoker's blood *p*-benzoquinone (*p*-BQ) derived from CS forms covalent adducts with cysteine 93 residues in both the β chains of hemoglobin (Hb) producing Hb-*p*-BQ adducts. UV–vis spectra and CD spectra analyses show that upon complexation with *p*-BQ the structure of Hb is altered. Compared to nonsmoker's Hb, the content of α-helix decreased significantly in smoker's Hb ($p = 0.0224$). *p*-BQ also induces aggregation of smoker's Hb as demonstrated by SDS-PAGE, dynamic light scattering and atomic force microscopy. Alteration of Hb structure in smoker's blood is accompanied by reduced oxygen binding capacity. Our results provide the first proof that *p*-BQ is a cause of hypoxia in smokers. We also show that although both *p*-BQ and CO are responsible for causing hypoxia in smokers, exposure to CO further affects the function over and above that produced by Hb-*p*-BQ adduct.

1. Introduction

Cigarette smoking has been identified as the most important source of morbidity and mortality worldwide. The Centers for Disease Control (CDC) estimate that smoking will result in death or disability for half of all people who continue to smoke [1]. Generally the life expectancy of smokers is nearly 14 years less than nonsmokers [2–5]. Apart from causing the various life-threatening diseases such as cancer of the lung and other organs, chronic obstructive pulmonary disease (COPD) and cardiovascular disease (CVD), cigarette smoke (CS) is also known to produce hypoxia [6,7]. In states of oxygen deficiency, the cells, tissues and the body as a whole are deprived of vital energy. Chronic hypoxia may be a cause of early aging, morbidity and premature death. Moreover, CS-related degenerative diseases such as cancer, COPD and CVD are likely to be further complicated by hypoxia resulting in shortening of life-span. Also, smoking during pregnancy causes reduced availability of oxygenated blood to the fetus resulting in intrauterine hypoxia and various risks for the unborn child [8–11]. However, the molecular mechanisms of cigarette smoke (CS)-induced hypoxia are not clear.

Cigarette smoke (CS) is a complex mixture of harmful chemicals, including long-lived semiquinones and carbon monoxide (CO) [12,13]. CO forms carboxyhemoglobin (COHb) in smoker's blood and this may be one of the mechanisms of hypoxia in heavy smokers [13]. However, the formation of COHb is a reversible process. The half-life of COHb of CO-poisoned patients treated with 100% oxygen at atmospheric pressure is about 74 ± 25 min [14]. Earlier we had shown that irrespective of the source, CS contains substantial amounts (100–200 μg/cigarette) of *p*-benzosemiquinone (*p*-BSQ) [15,16]. In the smoker's lung, *p*-BSQ is converted to *p*-benzoquinone (*p*-BQ), which is a strong arylating agent [17,18]. *p*-BQ produced in the smoker's lungs gets into the blood stream and forms covalent adducts with ε-amino groups of lysine residues of human serum albumin (HSA) [18]. This results in alteration of structure and ligand binding capacity of HSA [18]. Being a hydrophobic compound, *p*-BQ readily enters the cell [19]. We conceive that in the smoker's blood,

* Corresponding author at: Department of Biotechnology and Dr. B. C. Guha Centre for Genetic Engineering & Biotechnology, Calcutta University College of Science, 35, Ballygunge Circular Road, Kolkata 700019, India. Fax: +91 33 24614849.
E-mail address: ibc123@gmail.com (I.B. Chatterjee).

http://dx.doi.org/10.1016/j.toxrep.2016.02.001

p-BQ would enter into the red blood cells (RBC) and form covalent adduct with hemoglobin (Hb), which might result in alteration of its structure. The structure of Hb is so delicately balanced that small structural change such as modifications of internally located amino acid residues may render it nonfunctional for carrying oxygen [20]. We further envisage that the associated structural changes, if any, might alter the oxygen binding capacity, resulting in reduced oxygen delivery to the tissues leading to hypoxia. Since smokers are also exposed to CO [13], we were interested to see the interaction of CO with *p*-BQ on oxy-Hb.

2. Materials and methods

2.1. Materials

Human Hb was purchased from Sigma (H7379) and used without further purification. *p*-Benzoquinone (*p*-BQ) was obtained from Himedia (RM-489) and freshly crystallized from *n*-hexane before use. All other reagents used were of analytical grade. Affinity purified polyclonal antibody to *p*-BQ raised in rabbit after immunization with *p*-BQ-bovine serum conjugate was supplied by Abexome Biosciences, Bangalore, India. LC/MS- grade solvents, acetonitrile and formic acid were purchased from Fluka. RapiGest™. Sodium iodide (NaI), polyethylene glycol (PEG) mix and Glu-fibrino peptide B (GFP) were obtained from Waters (Milford, MA, USA). Trypsin was purchased from Sigma–Aldrich (St. Louis, MO, USA). Ammonium bicarbonate and ammonium acetate were purchased from Merck (India). All other reagents used were of analytical grade.

2.2. Ethics statement

The collection of human blood and subsequent experiments were approved by the Institutional Bioethics Committee for animal and human research studies, University of Calcutta, following the Code of Ethics of the World Medical Association (Declaration of Helsinki) for experiments involving humans. Written consents were obtained prior to collection of blood.

2.3. Preparation of *Hb*-p-*BQ adduct*

Hemoglobin was incubated with *p*-BQ in definite molar ratios (1:1, 1:2, 1:10, 1:20, 1:50) in 20 mM potassium phosphate buffer (pH 7.4) for two hours at 37 °C in the dark. The reaction mixture was dialyzed overnight at 4 °C to remove excess/free *p*-BQ and hydroquinone formed as a reaction product. The stock solution was diluted and used for subsequent experiments.

2.4. Isolation of hemoglobin from of human blood

Red blood cell (RBC) was isolated from whole blood using Ficoll-Paque™ PLUS reagent (Amersham Biosciences) following standard protocol and the pellet was washed with phosphate buffered saline (PBS) thrice. RBC was lysed by adding equal volume milliQ water to the pellet. The resulting solution was centrifuged at 20,000 × *g* for 15 min at 4 °C and the supernatant purified through PD-10 Desalting Column followed by Centricon centrifugation using 30 k Da membrane and the purified Hb was used for subsequent experiments.

For mass spectra analysis, Hb was isolated following the method described elsewhere [21]. Briefly, venus blood from smokers, collected in EDTA vial, was centrifuged at 1248 × *g* for 10 min at 25 °C. The obtained packed cells was washed with 0.9% NaCl thrice and then lysed with eight volumes of ice cold distilled water. The hemolysate was centrifuged at 12,880 × *g* for 10 min at 4 °C to remove the erythrocyte membranes. The Hb solution was then lyophilized, stored at −20 °C and used for mass spectroscopic analysis when needed.

2.5. Spectrophotometry of *Hb*-p-*BQ adduct*

The stock Hb solution prepared as described above was diluted to desired concentration and the absorbance was measured from 200 to 700 nm in a Shimadzu UV-2540 spectrophotometer. For time-dependent measurement of Hb-*p*-BQ interaction, Hb was incubated with *p*-BQ at a molar ratio of 1:50.

2.6. Mass spectrometric analysis of *Hb*-p-*BQ adduct A. Intact protein analysis*

Samples were prepared and dialyzed overnight against 10 mM ammonium acetate, pH 7.4. Immediately before the mass spectroscopic analysis, the lysate was diluted to a concentration of 25 μM in 10 mM ammonium acetate, pH 7.4. Using gold coated borosilicate capillaries, the sample was infused into nano-ESI source of Synapt HDMS mass spectrometer (Waters, Manchester, UK). Data were acquired in positive ion mode with a capillary voltage of 1.9 kV in the *m*/*z* range 650–5000. TOF analyzer was calibrated using cesium iodide (2 mg/ml) in 50% aqueous 2-propanol. The instrument acquisition parameters were adjusted to obtain optimal signals. The sampling and extraction cone voltages were set to 100 V and 2 V respectively. Source temperature was maintained at 37 °C and the gas flow was set at 1.5 ml/min. The backing pressure was increased to 5.9 m bar for better transmission of large protein assemblies aided by collisional cooling. Data were acquired and processed with MassLynx v4.1 software (Waters, UK).

2.7. Globin chain analysis

2 μg of hemolysate protein was injected through a C18 RP analytical column (ZORBAX Eclipse, 150 mm × 4.6 mm, 3.5 μm) at room temperature. Globin chains were eluted using a linear gradient of 2% increase in acetonitrile per minute containing 0.1% acetic acid at a flow rate of 0.2 ml/min and the mass analysis was performed on Synapt HDMS with electrospray ionization (ESI) source (Waters). The data were acquired in positive ion 'V' mode over the range of 650–1500 *m*/*z*, with a capillary voltage of 3 kV using a source temperature of 120 °C and desolvation gas temperature of 350 °C. The mass calibration was done using NaI. The mass spectrum was smoothed, baseline subtracted, and subsequently deconvoluted using MaxEnt1 software. Since the charge state distributions of β-globin chain and its adducts were observed to be identical in mass spectra, the respective signal intensities of different molecular ions were correlated with their relative abundance. The most intense signals of the observed protonated populations, namely, β, glycated-β, glutathionylated-β and pBQ adduct of the β-globin chain were found to be distributed across the charge states from 11 to 19. Thus the quantification of each population of β-globin adducts was calculated as follows:

$$p\text{BQ} - \beta \text{ adduct of hemoglobin\%} = \frac{p\text{BQ adduct of } \beta \times 100}{(\beta + \text{Hb}\beta - \text{gly} + \text{Hb}\beta - \text{GS} + p\text{BQ adduct of } \beta)} \quad (1)$$

$$\text{Hb}\beta - \text{gly\%} = \frac{\text{Hb}\beta - \text{gly} \times 100}{(\beta + \text{Hb}\beta - \text{gly} + \text{Hb}\beta - \text{GS} + p\text{BQ adduct of } \beta)} \quad (2)$$

$$\text{Hb}\beta - \text{GS\%} = \frac{\text{Hb}\beta - \text{GS} \times 100}{(\beta + \text{Hb}\beta - \text{gly} + \text{Hb}\beta - \text{GS} + p\text{BQ adduct of } \beta)} \quad (3)$$

2.7.1. Proteolytic digestion

Hb modified with *p*-BQ in the molar ration 1:2 was digested with proteolytic enzyme trypsin. Modified Hb was denatured by incubating 10 μg of protein with 1 μl of 0.2% RapiGest™ in 50 mM NH_4HCO_3 (pH 7.8) at 80 °C for 15 min. Following denaturation, proteolytic digestion was performed at 37 °C overnight using trypsin as proteolytic enzyme, at a ratio trypsin:hemoglobin 1:10 (w/w). To break down RapiGest™, the digested sample was acidified with 1 μl of formic acid (FA) and incubated at 37 °C for 90 min. It was then centrifuged at 6000 rpm for 20 min and supernatant was taken for mass spectrometry based proteomics analysis.

2.7.2. nLC/ESI-MS

Digested protein (100 fmol) was loaded onto a nano Acquity UPLC 1.7 μm BEH130C18 column (250 mm × 75 μm) at 35 °C. Peptides were eluted with a gradient of 3–40% of solvent B over 60 min using a flow rate of 300 nl/min, where solvents A and B consisted of water and acetonitrile with 0.1% FA, respectively. The eluted peptides were analyzed in Synapt HDMS (Waters, UK) coupled to nano Acquity UPLC. The data were acquired in the mass range 50–1600 m/z using the MS^E mode of acquisition. Reference compound GFP was continuously infused through lockspray and scanned every 45 s. MS calibration was done with GFP. The data was analysed using PLGS 2.5 software.

2.8. Circular dichroism (CD) analysis

Far UV-CD spectra of Hb and Hb-*p*-BQ adduct was recorded on a Jasco J720 spectropolarimeter by scanning reaction mixtures from 190 to 250 nm using 1 mm path length cuvette. Mean residual ellipticity (MRE) was calculated using the formula, MW = [Observed(θ)]/[10 × C_p × n × l] in deg cm^2 $dmol^{-1}$, where θ is the observed ellipticity in millidegree, MW is the molecular weight in k Da, C_p is the molar concentration, n is the number of amino acids and l is the path length in cm. The α-helix percentage was calculated using MRE value at 222 nm according to the formula [(MRE-2340)/30300] × 100 [22].

2.9. Dynamic light scattering (DLS)

Nano-ZS (Malvern) instrument (5 mW HeNe laser λ, 632 nm) was used for photon correlation spectroscopy. The samples (0.25 mg/ml) were poured into a DTS0112 low-volume disposable sizing cuvette of 1.5 ml (path length 1 cm) after passing through a 0.22 μm filter. Using the DTS software supplied with the instrument, the operating procedure was programmed to record average of 30 runs, each run being averaged for 15 s. A particular Stokes radius (Rh) was computed in each case and the result ultimately presented as the size distribution by numbers of Rh.

2.10. Atomic force microscopy (AFM)

Human Hb (Sigma), Hb-*p*-BQ adduct prepared from Hb and also Hb isolated from blood (smokers/nonsmokers) were dissolved in 20 mM ammonium bicarbonate buffer (pH 7.4) (10 μl of 1 μM solution) and deposited onto freshly cleaved muscovite Ruby mica sheet (ASTM V1 Grade Ruby Mica from MICAFAB, Chennai) and dried for 5–10 min at room temperature. Tapping mode AFM was performed using a Pico plus 5500 AFM (Agilent Technologies USA) with a piezoscanner of maximum range up to 9 μm. Micro fabricated silicon cantilevers of 225 μm in length with a nominal spring force constant of 21–98 N/m were used from Nano sensors. Cantilever oscillation frequency of 275.1 kHz was tuned into resonance frequency. The images (256 by 256 pixels) were captured with a scan size between 0.5 and 3 μm at the scan speed rate of 0.499 lines/s or 0.474 μm/s. Images were processed using Pico view 1.10.1 (9995) software (Agilent Technologies, USA). Length, height and width of Hb and Hb-*p*-BQ adducts were measured manually using Pico view 1.10.1 (9995) software.

2.11. Assay of oxygen uptake by Hb

Analysis of oxygen uptake by Hb (10 nmoles of Hb in 2 ml of MIli-Q water), isolated from smokers and nonsmokers as described above, was carried out using Gilson Oxygraph (Gilson Medical Electronics, Middleton, Wisconsin). Parallel experiments were carried out using pure human Hb (Sigma–Aldrich) before and after conjugation with *p*-BQ.

2.12. Interaction of CORM-3 (carbon monoxide releasing molecule) with p-BQ on oxy-Hb

The release of CO from CORM-3 [tricarbonylchloro(glycinato)ruthenium(II)] was assessed spectrophotometrically by measuring conversion of oxy-Hb to carboxyhemoglobin (HbCO). Hb (5 mM) isolated from nonsmoker's blood was treated with dithionite (0.1%) to reduce any MetHb present followed by vortexing in air to produce oxy-Hb according to the method described elsewhere [23]. To study the effect of CORM-3 on oxy-Hb, 10 ml aliquots from a stock solution of CORM-3 (50 mM) were added to a cuvette containing 5 mM oxy-Hb in potassium phosphate buffer, pH 7.4 and absorption spectrum was recorded in triplicate in a spectrophotometer (Shimadzu UV-2540). Successive additions of CORM-3 were made to reach final CORM-3 concentrations of 0.5, 1.0, 1.5, 2.0 and 4.0 mM. The amount of HbCO formed was calculated from the difference of soret peak of human oxy-Hb at 415 nm ($e^{HbO2}{}_{415\,nm}$ = 128 mM^{-1} cm^{-1} [24], before and after addition of CORM-3 following the method of Antonini and Brunori [25].

To study the effect of *p*-BQ on CORM-3 treated oxy-Hb, 2 mM CORM-3 (final concentration) was added to a cuvette containing 5 mM oxy-Hb in potassium phosphate buffer, pH 7.4 and absorbance was recorded after 5 min. Then 10.8 μg *p*-BQ was added to the cuvette to obtain Hb:*p*-BQ in a molar ratio of 1:20 and absorbance spectrum was recorded after 5 min.The experiment was repeated using 4.0 mM CORM-3 (final concentration).

The effect of CORM-3 on Hb-*p*-BQ conjugate was studied by adding different concentrations of CORM-3 (final, 0.5, 1.0, 2.0 and 4.0 mM, respectively) to 5 mM oxy-Hb:*p*-BQ (in molar ratio 1:20) in potassium phosphate buffer, pH 7.4. Absorption spectrum for each CORM-3 final concentration was recorded in triplicate. The effect of CORM-3 was calculated on the basis of difference of absorbance at soret peak of *p*-BQ-oxy-Hb conjugate at 413 nm following the method of published elsewhere [25].

2.13. Statistical calculation

All values are expressed as mean ± SD. Statistical significance was carried out using one way ANOVA. The *p*-values were calculated using appropriate *F*-tests. Difference with *p*-values <0.05 was considered significant.

3. Results

3.1. Identification and characterization of Hb-p-BQ adduct in smoker's blood

Using antibody against *p*-BQ, here we show by immunoblot that smoker's blood contains Hb-*p*-BQ adduct (Fig. 1A). Quantitation of immunoblots (Fig. 1B) shows that moderate smokers (≈15 cigarettes/day for 15–20 years) have significantly more (p = 0.0000)

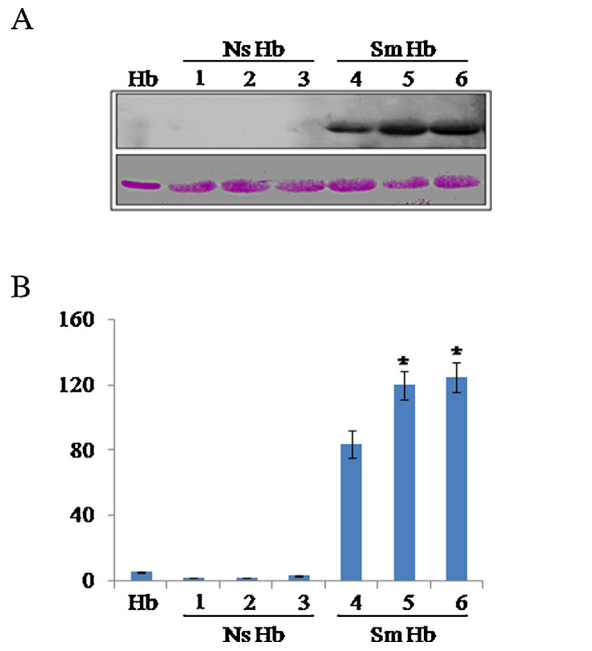

Fig. 1. Representative immunoblots of pure Hb and Hb isolated from blood of smokers (Sm Hb) and nonsmokers (Ns Hb) (male, 45–55 years) showing Hb-*p*-BQ adducts. (A) Hb, pure Hb; NS Hb, Hb isolated from blood of nonsmokers; Sm Hb, Hb isolated from smokers. Sm Hb 4, mild smoker (≈10 cigarettes/day for 15–20 years); Sm Hb 5, 6, moderate smokers (≈15 cigarettes/day for 15–20 years). (B) Quantitation of immunoblots using NIH image J. * indicates significant increase ($p = 0.0000$) in Hb-*p*-BQ adduct in blood of moderate smokers compared to mild smokers. Fifteen μg protein was loaded in each lane.Bottom panel, ponceau S staining as the loading control.

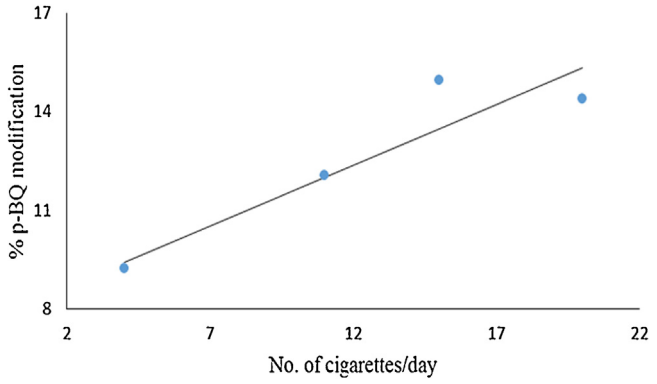

Fig. 2. The best fit line indicating increase in relative abundance of *p*-BQ adduct of hemoglobin *in vivo* with increase in the number of cigarettes smoked per day.

Hb-*p*-BQ adduct than that of mild smokers (≈10 cigarettes/day for 15–20 years).

We analyzed Hb and its adducts present in smoker's blood using LC/ESI-MS platform. Mass analyses of different globin polypeptide chains indicated the presence of three major adducts of β-globin chain, namely, glutathionylated β (16172 Da), glycated β (16028 Da) and *p*-BQ adduct of β chain (15973 Da) (Supplementary Fig. 1). There was no *p*-BQ adduct observed in α-globin chain.

The relative abundance of *p*-BQ adduct of β-globin chain was calculated in the four smoker's blood samples as described in methods. Although there were variations in the age and years of smoking across different subjects, we attempted to correlate the number of cigarettes smoked per day by each individual with quantified values of *p*-BQ adduct of β-globin chain. An increasing trend in the relative abundance of *p*-BQ adduct was observed with the increase in the number of cigarettes smoked per day (Fig. 2). The *p*-BQ adduct of the β-globin chain in smokers blood was calculated as mentioned under Materials and Methods. The percentages of *p*-BQ adduct was found to be 9.22%, 12.05%, 14.93%, 14.37% for inviduals who smoked 4, 11, 15 and 20 cigarettes per day respectively (Fig. 2).

On incubation of nonsmoker's human Hb with *p*-BQ *in vitro* at physiological pH and temperature showed the formation of a covalent adduct in the hemoglobin tetramer. Fig. 3, panel A shows the mass spectra of non-covalently bound four globin chains alongwith their respective heme units. The appearance of different peaks with *m*/*z* (+z) at 3404.3 (+19), 3593.5 (+18) and 3804.8 (+17) shows the presence of a molecular ion of mass 64665 Da. The calculated stoichiometry obtained from the masss analysis of Hb adduct indicates the presence of two *p*-BQ moieties per Hb tetramer $[(\alpha^h)_2(\beta_{pBQ}{}^h)_2]$. Additionally, we observed the glutathionylated adduct of the aforementioned molecular ion having low intensity at 64970 Da. Fig. 3 panel B shows the mass spectra of *p*-BQ adduct of the tetramer $[(\alpha^h)_2(\beta_{pBQ}{}^h)_2]$ in different globin chains synthesized *in vitro*. Fig. 3 panel C shows the following masses of the different globin chains: α (15126 Da), β (15867 Da) and β_{pBQ} (15972 Da). The mass analyses of both tetramer and monomer indicated that *in vitro* modification of Hb with *p*-BQ results in incorporation of one *p*-BQ moiety per β-globin chain. The αglobin chain did not undergo any modification.

Bottom-up proteomics approach was used to identify the site of modification on the β-globin chain. The *p*-BQ adduct of Hb synthesized *in vitro* was subjected to proteolysis using trypsin as the proteolytic enzyme. The tryptic digest was analysed using nano LC-MS^E method and the obtained data was processed using PLGS 2.5 software and searched against normal human Hb database with *p*-BQ as modifying agent. The proteomics analysis identified the peptide fragment (charge—4+, precursor rms mass error—17.44 ppm, PLGS score—7.96) consisting of residues 85–102 of β-globin chain carrying a *p*-BQ moiety covalently bonded to Cys-93.

3.2. Spectrophotometric analysis of Hb-p-BQ adduct

The formation of Hb-*p*-BQ adduct was monitored by changes in the absorption spectrum at different molar concentrations of Hb:*p*-BQ and also in a time-dependent manner. Pure Hb spectrum exhibited two peaks, one at 414 nm corresponding to the Soret band and another peak around 273 nm characterizing the aromatic amino acids present in the Hb molecule. Hb was incubated with *p*-BQ at different molar ratios and dialyzed overnight to eliminate any excess/free *p*-BQ and hydroquinone formed as a reaction product. Examination of the reaction mixtures revealed that compared to pure Hb, there was a decrease in the Soret band of Hb-*p*-BQ adduct. The decrease was about 1.5%, 10.34%, 15.50% and 19.38% in Hb-pBQ adduct produced in the molar ratios of 1:1, 1:10, 1:20 and 1:50, respectively. This alteration was accompanied by an increase in absorbance at 350 nm corresponding to the formation of *p*-BQ adduct as reported earlier [18] (Fig. 4). Time-dependent interaction between Hb with *p*-BQ at molar ratio of 1:50 revealed similar reduction in the Soret band. The absorbance reduced significantly to 26.18% ($p = 0.0000$, $n = 3$) after two hr incubation with consequent increase in absorbance at 350 nm indicating augmented formation of *p*-BQ adduct (Fig. 5). Fig. 6 shows that there is a significant decrease of Soret band of about 16.6% ($p = 0.0000$) of smokers Hb (0.346 ± 0.001, $n = 6$) compared to nonsmoker's Hb (0.425 ± 0.001, $n = 6$).

3.3. Alteration in the secondary structure of Hb after interaction with p-BQ

The alteration of secondary structure was investigated using far UV-CD. Spectropolarimetric analysis of pure Hb elucidated negative ellipticity at 208 nm and 222 nm indicating a primarily α-helical

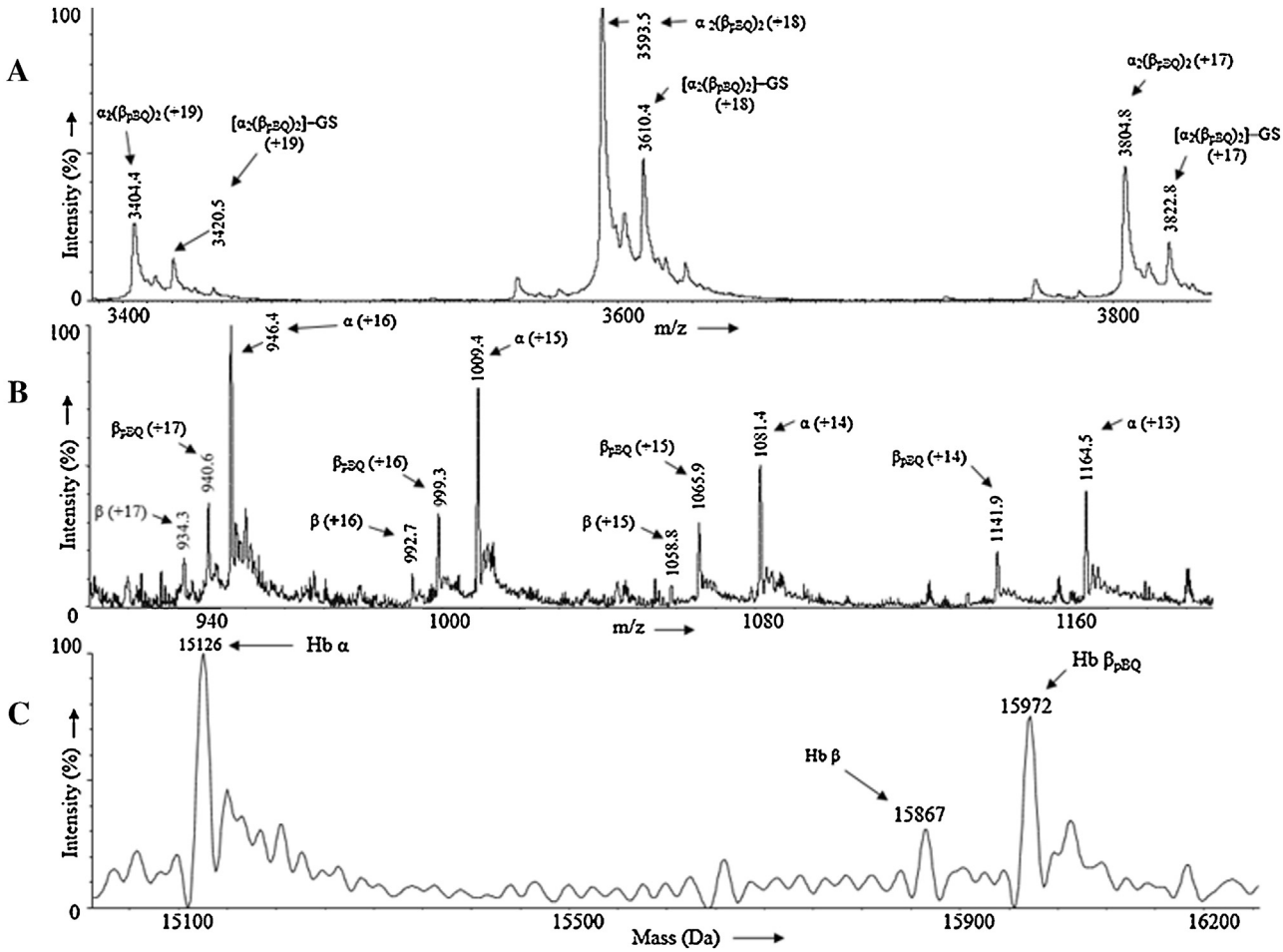

Fig. 3. (A) Mass spectrum of non-covalently bound four globin chains alongwith their respective heme units. (B) Mass spectrum of the different globin chains present in *p*-BQ adduct of the tetramer $[(\alpha^h)_2(\beta_{pBQ}{}^h)_2]$ synthesized *in vitro*. (C) Deconvoluted mass spectrum of the different globin chains: α (15126 Da), β (15867 Da) and β_{pBQ} (15973 Da).

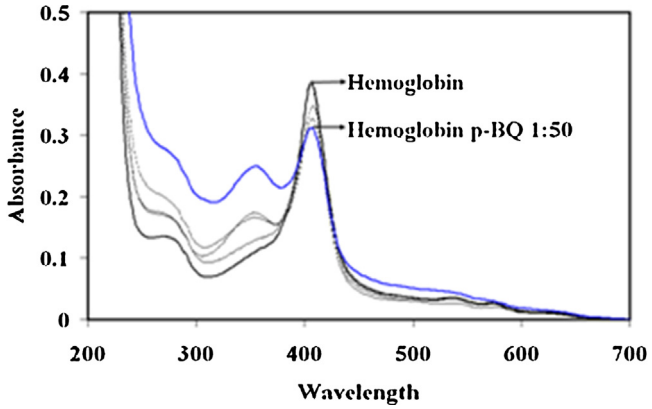

Fig. 4. Absorption spectra of Hb and HB-*p*-BQ adducts at different molar ratios of Hb:*p*-BQ (1:1–1:50) showing gradual decrease of Soret band at 414 nm accompanied by increase in absorption at 350 nm indicating formation of Hb-*p*-BQ adduct.

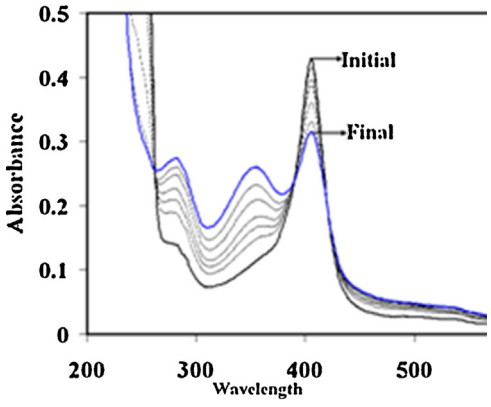

Fig. 5. Absorption spectra of Hb and HB-*p*-BQ adducts at molar ratios of Hb:*p*-BQ (1:50) at different time intervals of incubation showing gradual decrease of Soret band at 414 nm accompanied by increase in absorption at 350 nm, indicating formation of Hb-*p*-BQ adduct.

conformation. In the Hb-*p*-BQ adduct prepared at molar ratio of 1:50, the Hb molecule showed an overall decreased ellipticity and the percentage of α-helix content decreased significantly from 83.79 ± 0.7 to 72.4 ± 1.6 ($p = 0000$) (Fig. 7). The Hb isolated from smoker's blood also showed a decreased ellipticity indicating loss of secondary structure compared to the Hb from nonsmoker's blood (Fig. 8). The content of α-helix (73.92% ± 4.8) decreased significantly ($p = 0.0224$, $n = 6$) in smoker's Hb compared to that (81.88% ± 5.40) of nonsmoker's Hb.

3.4. Aggregation of Hb molecules after interaction with p-BQ

p-BQ is known to form cross-links and aggregation of proteins [26,27]. Using SDS-PAGE we demonstrated that interaction of Hb with *p*-BQ in concentration-dependent and time-dependent manner produced Hb aggregation (Fig. 9A, B). Our results also show that compared to nonsmoker's Hb, smoker's Hb contains aggregated Hb (Fig. 9C).

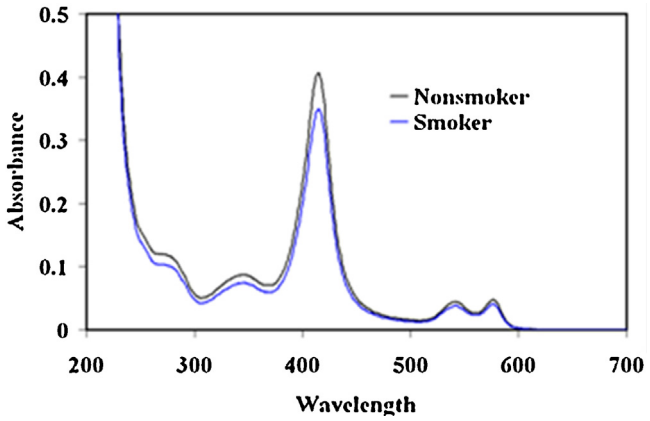

Fig. 6. Decrease in Soret band of Hb isolated from blood of moderate smokers compared to nonsmokers.

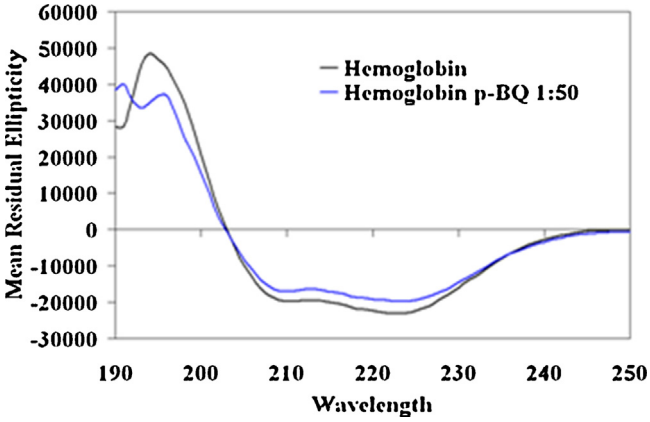

Fig. 7. Far UV CD spectra of Hb and Hb-*p*-BQ adduct at a molar ratio of 1:50, showing change in the secondary structure.

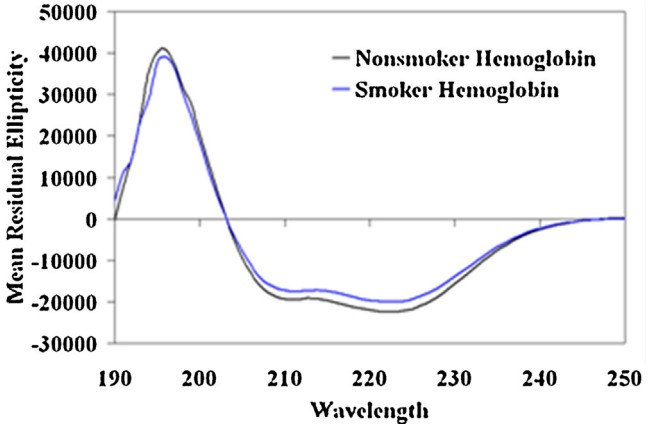

Fig. 8. Representative far UV CD spectra of Hb isolated from blood of moderate smokers compared to nonsmokers showing change in the secondary structure.

To investigate the change in the molecular radius of hemoglobin after conjugation with *p*-BQ, we employed dynamic light scattering (DLS) technique to quantify the size of the protein. The molecular radius of pure hemoglobin was 4.85 nm, which was in good agreement with the previously published result [28]. The increased radius of Hb as measured by DLS showed continuous rising trend with increasing molar concentrations of *p*-BQ indicating probable formation of Hb aggregates after interaction with *p*-BQ. The calculated molecular radii were 6.5 nm, 11.7 nm, 18.2 nm and 24.4 nm for Hb-*p*-BQ adducts in the molar ratios of 1:1, 1:10, 1:20 and 1:50, respectively (Fig. 10A). When the molecular size of Hb from nonsmokers' blood and that of smokers was compared, the smoker's Hb showed a radius of 18.4 ± 1.7 nm while that of nonsmoker, 6.8 ± 0.7 nm (Fig. 10B). The aggregation of Hb in smoker's blood was also confirmed by atomic force microscopy (Fig. 11A, B).

3.5. Oxygen binding capacity of Hb-p-BQ adduct

The alteration of structure and aggregation of smoker's Hb was accompanied by loss of oxygen (O_2) binding capacity. When the O_2 binding capacity of pure Hb (38.96 ± 1.4 nmol O_2/10 nmol Hb) was compared with that of Hb-*p*-BQ adducts prepared at different molar concentrations of *p*-BQ, O_2 uptake was gradually lost in a concentration-dependent manner (Fig. 12A). The values were 36.6 ± 1.4 ($p = 0.100$), 24.7 ± 1.4 ($p = 0.002$), 14.3 ± 2.4 ($p = 0.001$) and 8.8 ± 1.4 ($p = 0.000$) at Hb:*p*-BQ molar ratios of 1:1, 1:10, 1:20, 1:50, respectively (Fig. 12A). Fig. 12B further shows that the oxygen uptake of smoker's Hb (31.0 ± 1.1 nmoles of O_2/10 nmoles Hb) is significantly less ($p = 0.0000$) than nonsmoker's Hb (36.6 ± 1.4 nmolof O_2/10 nmoles.

3.6. Interaction of CORM-3 with p-BQ on oxy-Hb

We have shown in this paper that *p*-BQ derived from CS produces Hb-*p*-BQ adduct in smokers that is accompanied by alteration of structure and function of Hb. It is also well established that smokers are exposed to CO as revealed by the formation of HbCO [13]. We were therefore interested to see how CO affects *p*-BQ modification of oxy-Hb and vice versa. We simultaneously exposed oxy-Hb to CORM-3 (a water soluble CO releasing molecule) and *p*-BQ, a situation supposed to be happening *in vivo*. Fig. 13A shows that treatment of 5 μM nonsmoker's oxy-Hb with 0.5, 1.0, 1.5, 2.0 and 4.0 μM CORM-3 produced 1.96 ± 0.28, 3.37 ± 0.14, 4.91 ± 0.28, 5.75 ± 0.28 and 9.12 ± 0.14 SD %HbCO, respectively. A cohort study indicates that in chronic smokers the %HbCO may vary from 6.02% to 9.6 [13]. Fig. 13B shows that additions of 2.0 and 4.0 μM CORM-3 that produce 4.91 and 9.12%HbCO, respectively, cause significant decrease ($p = 0.000$) in the soret peak (415 nm) of oxy-Hb. Under the condition, addition of *p*-BQ to the incubation medium does not further affect the soret band. Also, when CORM-3 was added to oxy-Hb-*p*-BQ conjugate in the incubation medium, 2.0 and 4.0 μM CORM-3 produced significant decrease ($p = 0.002$ and 0.001, respectively) in soret band (413 nm) (Fig. 11C). The results indicate that CO affects the function of oxy-Hb in smokers over and above that produced by *p*-BQ.

4. Discussion

In this paper we have demonstrated by immunoblot and mass spectrometry that smoker's blood contains Hb-*p*-BQ covalent adducts with −SH groups of cysteine residues (Cys93) of the β-globin chain of Hb. Using UV–vis spectroscopy, CD, SDS, DLS and AFM, we have also shown that formation of *p*-BQ adducts is accompanied by alteration of structure and aggregation of Hb, leading to reduced oxygen binding capacity. Using CORM-3, a CO releasing molecule, we have further shown that *p*-BQ affects the function of oxy-Hb over and above that produced by CO.

Quantitation of immunoblots indicate that the content of Hb-*p*-BQ adduct is significantly greater ($p = 0.000$, $n = 10$) in moderate smokers (15–20 cigarettes/day for 15–20 years) than that of mild smokers (≈10 cigarettes/day). In a different subset of four smokers, mass spectrometry based relative quantification of *p*-BQ adduct of β-globin chain showed the presence of increasing amount of the adduct with increase in number of cigarettes smoked.

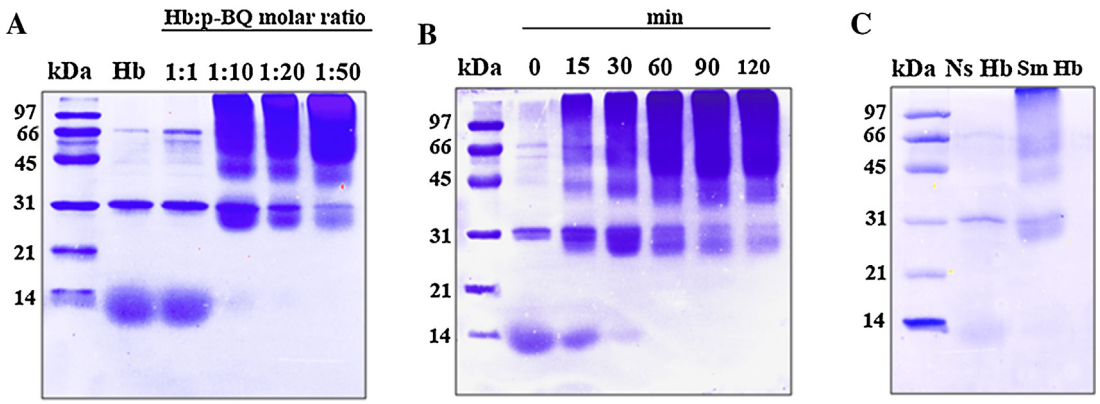

Fig. 9. SDS-PAGE of pure Hb, Hb-*p*-BQ adducts and Hb isolated from nonsmokers (Ns) and smokers (Sm). (A) Pure Hb and Hb-*p*-BQ adducts at different molar ratios. (B) Hb-*p*-BQ adduct at molar ratio of 1:50 at different time points of incubation at 37 °C in 20 mM potassium phosphate buffer, pH 7.4. (C) Representative SDS-PAGE of Hb isolated from Ns and Sm. Experiments were done with 6 samples each of Ns and Sm. Loading of Hb in each lane was 50 μg in A & B and 30 μg in C in a 14% gel; stained with Coomasie Brilliant Blue-R250. The upper portion of each lane shows aggregation of Hb. Details are given under Section 2.

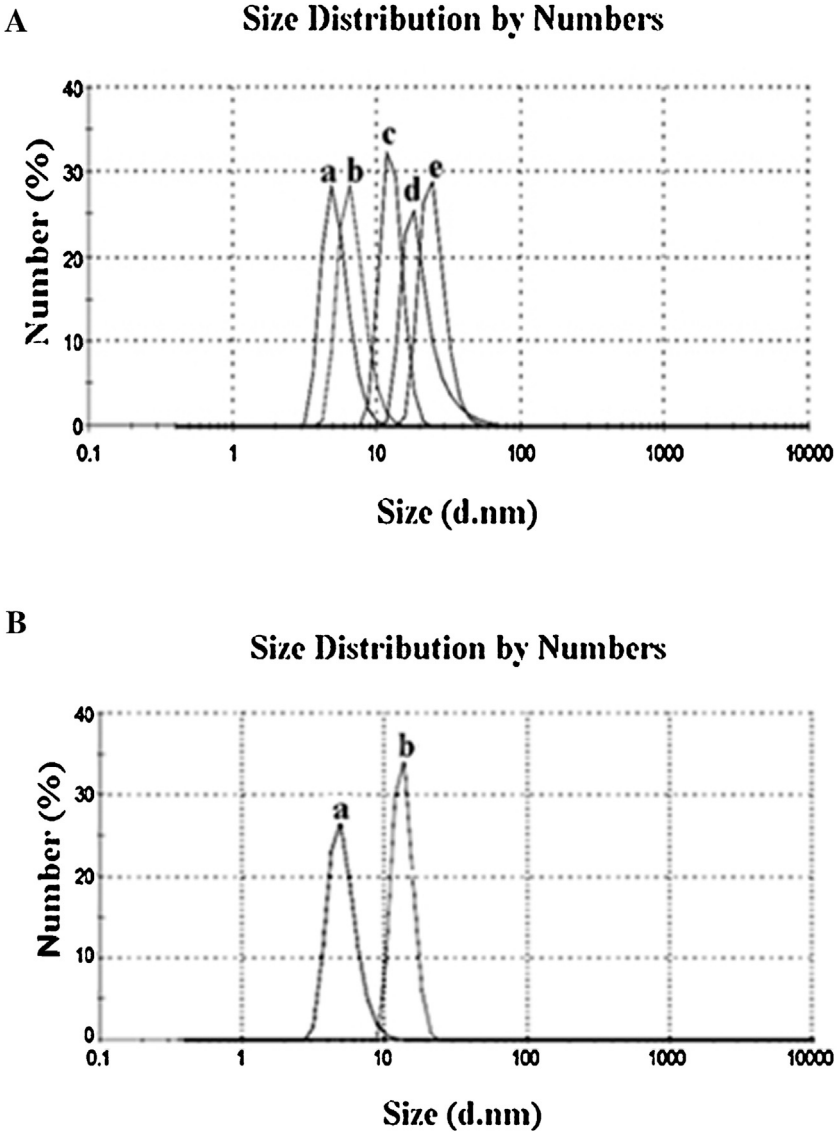

Fig. 10. (A) DLS analysis of hemoglobin before and after reaction with different concentrations of *p*-BQ. a,b,c,d and e represent Hb-*p*-BQ adduct at molar ratio of 1:0, 1:1, 1:10, 1:20 and 1:50, respectively. (B) Representative picture of DLS analysis of hemoglobin extracted from blood of (a) nonsmoker and (b) moderate smokers.

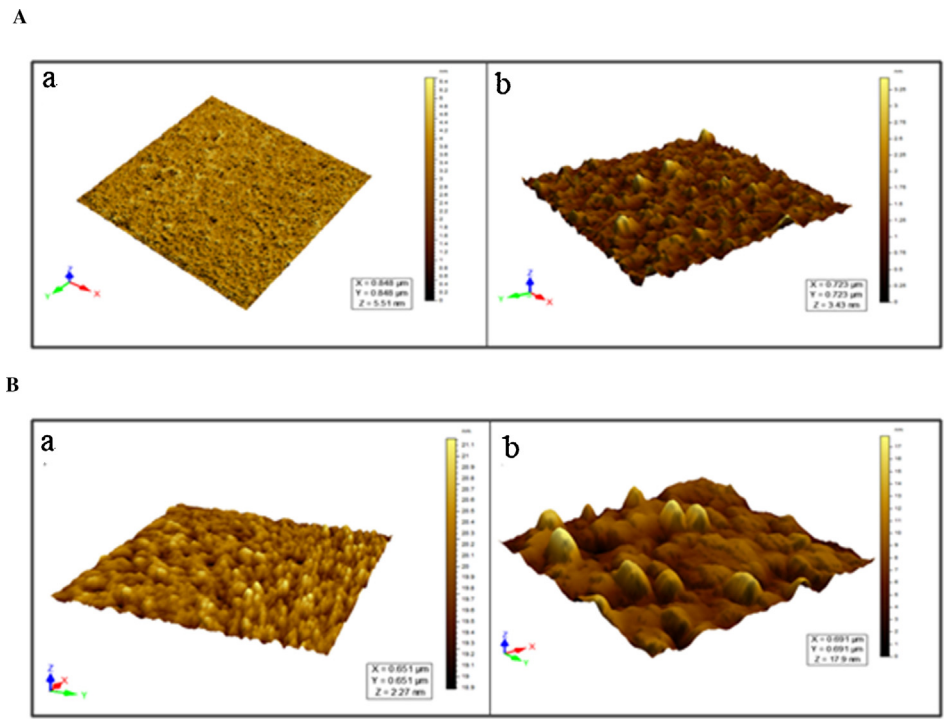

Fig. 11. (A) Atomic Force Micrographs of (a) Hb and (b) Hb-*p*-BQ adduct at a molar ratio of 1:50. (B) Representative Atomic Force Micrographs of Hb isolated from (a) nonsmokers and (b) moderate smokers.

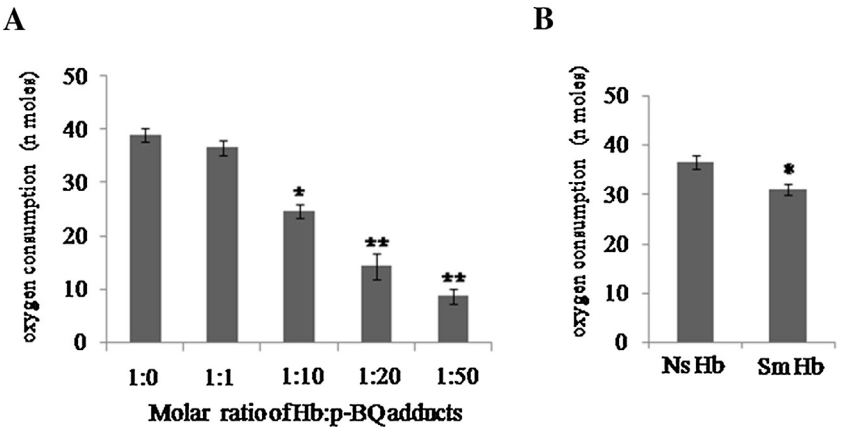

Fig. 12. (A) Oxygen consumption by Hb-*p*-BQ adduts at different molar ratios of Hb:*p*-BQ, *indicates highly significant (*$p = 0.0002$, **$p = 0.0000$) compared to pure Hb; (B) Representative oxygen consumption by Hb isolated from blood of smokers (Sm) and nonsmokers (Ns). *indicates highly significant ($p = 0.0000$; $n = 10$; CI 95% Ns: 35.4–37.8; Sm, 29.9–32.2).

Human adult hemoglobin is a tetrameric protein consisting of α and β-globin chains in duplicate where α-globin subunit has one cysteine residue (Cys104) and β-globin subunit has two cysteine residues (Cys93, Cys112). Among those three cysteine residues βCys93 is 5-fold more accessible compared to βCys112, whereas αCys104 is completely buried [29].

Mass analysis of *in vitro p*-BQ adduct of hemoglobin in its tetrameric form showed the presence of two *p*-BQ moieties per tetramer. Subsequent mass analysis of individual globin chains revealed that in the *in vitro* adduct, a single modification occurred on each β-globin chain with α subunit remaining unmodified. Proteomics analysis of *in vitro p*-BQ adduct of hempglobin confirmed βCys93 is the site of modification in Hb. This covalent modification probably perturbs the conformation of the molecule resulting in disruption of some potential salt bridges at the $\alpha_{1\beta2}$ and $\alpha_{2\beta1}$ interfaces. Far-UV CD analysis indicated that conjugation with *p*-BQ altered the secondary structure of smoker's Hb. The content of α helix decreased significantly ($p < 0.05$).

Interaction of Hb with *p*-BQ not only produce covalent adduct but also cross-linking and aggregation of Hb. SDS-PAGE analysis, DLS studies as well as AFM indicate that *p*-BQ forms Hb aggregates and that smoker's blood contains aggregated Hb.

It is reported that *p*-BQ forms 1, 4 Michael adduct with thiol groups of proteins [30]. Nucleophilic additions of *p*-BQ at two different sites with the sulfhydryl groups of βCys93 of two different Hb molecules might lead to cross-linking between tetramers and aggregation of Hb molecules in smoker's blood. Alteration of the structure of Hb along with aggregation could be the cause of reduced uptake of oxygen by smoker's Hb.

Smoking during pregnancy can lead to a plethora of health risks to both the mother and the fetus [8–11]. Smoking in pregnancy accounts for an estimated 20–30% of low birth weight babies, up to

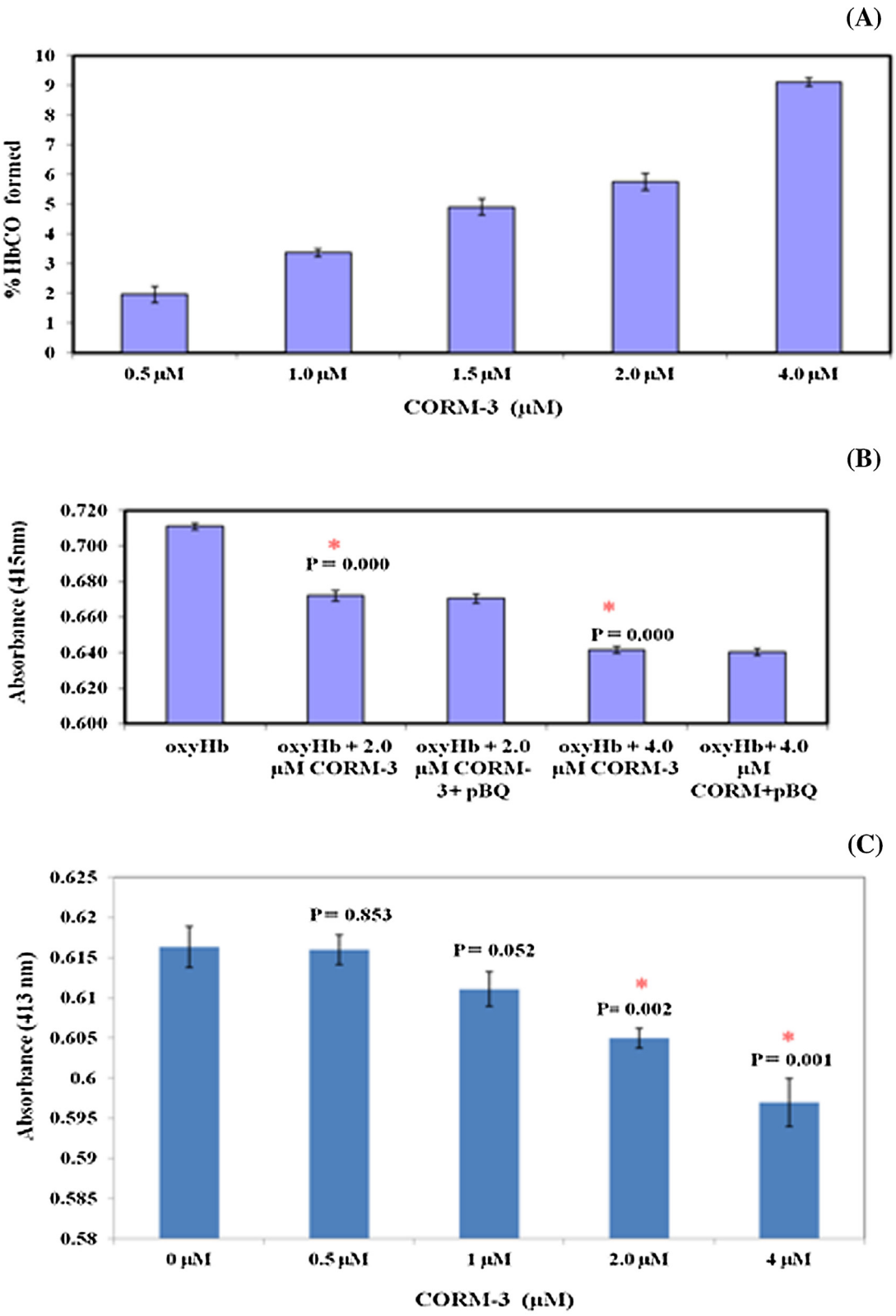

Fig. 13. Interaction of CORM-3 (carbonmonoxide releasing molecule) with *p*-BQ on oxy-Hb. (A) Formation of %HbCO after addition of CORM-3 to oxy-Hb. Aliquots from a stock solution of CORM-3 (50 mM) were added successively to 5 mM oxy-Hb isolated from nonsmoker's blood to attain final CORM-3 concentrations of 0.5 mM, 1.0 mM, 1.5 mM, 2.0 mM and 4.0 mM. Absorbance were recorded in triplicate at 200–700 nm after 5 min of each CORM-3 addition; %HbCO was calculated as means ± SD. Details are given in Materials and Method Section. (B) Effect of *p*-BQ on CORM-3 treated oxy-Hb. Aliquots of CORM-3 were separately added to 5 mM oxy-Hb isolated from nonsmoker's blood to attain final CORM-3 concentrations of 2.0 mM and 4.0 mM, respectively. Five min after addition of CORM-3, %HbCO obtained from these two concentrations were 5.75% ± 0.28 SD and 9.12% ± 0.14 SD, respectively. This was followed by addition of *p*-BQ (10.8 mg) to obtain Hb:*p*-BQ molar ratio of 1:20. Five min after addition of *p*-BQ, absorbance spectra were recorded in triplicate; * indicates significant difference of soret peak (at 415 nm) with respect to untreated oxyHb. Details are given in Section 2. (C) Effect of CORM-3 on oxy-Hb-*p*-BQ adduct. To 5 mM oxy-Hb-*p*-BQ adduct (in the molar ratio of 1:20) CORM-3 was added in aliquots form a stock solution of 50 mM to attain final CORM-3 concentrations of 0.5 mM, 1.0 mM, 2.0 mM and 4.0 mM, respectively. 5 min after addition of each CORM-3 concentration, absorbance spectra were recorded in triplicate; * indicates significant difference of soret peak (at 413 nm) with respect to untreated oxy-Hb:*p*-BQ adduct. Details are given in Section 2.

14% of preterm deliveries, and some 10% of all infant deaths. Even apparently healthy, full-term babies of smokers have been found to be born with narrowed airways and reduced lung function [10]. A recent study conducted in the United Kingdom found that smokers were five times more likely to develop pre-eclamsia [31].

It is well established that smokers are exposed to CO and a mechanism of hypoxia is formation of HbCO [13]. We have shown in this paper that another cause of hypoxia in smokers is formation of Hb-*p*-BQ adduct. *p*-BQ binds with cysteine residues of Hb and this binding is covalent and irreversible. On the other hand, the binding of CO with Hb is reversible [13]. Nevertheless, the affinity between Hb and CO is approximately 230 times stronger than the affinity between Hb and oxygen [32]. Hb binds to CO in preference to oxygen, resulting in less release of oxygen in the tissues. We have shown that exposure of oxy-Hb-*p*-BQ to CORM (a carbon monoxide releasing molecule) results in significant decrease in the soret band of oxy-Hb-*p*-BQ. This would indicate that although both *p*-BQ and CO are responsible for causing hypoxia in smokers, exposure to CO further affects the function of Hb-*p*-BQ.

5. Conclusions

In conclusion, we demonstrated that in smokers *p*-BQ derived from cigarette smoke forms covalent adducts with cysteine 93 residues in both the β chains of Hb producing Hb-*p*-BQ adducts. The formation of *p*-BQ adducts is accompanied by alteration of the structure and aggregation of Hb, leading to reduced oxygen binding capacity. Our results provide the first proof that *p*-BQ is a cause of hypoxia in smokers.

Conflict of interest

The authors declare that they do not have any conflict of interest.

Contributors

IBC conceived and designed major part of the experiments. RB designed part of the experiments on biophysical studies. AG performed a major part of the experiments. BR did some biophysical studies. SB did experiments on CORM studies and oxygen binding capacity. IBC, RB and AKM analyzed the data. Contributed reagents/materials/analysis tools: IBC, AKM. Wrote the paper: IBC and AM. AM, MM and AKM carried out the mass spectra analyses.

Funding

This research was supported by the Juthika Research Foundation, Krishna and Suhkamay Lahiri Cancer Research Foundation and Phulrenu Guha Research Fellowship of the University of Calcutta.

Transparency document

The Transparency document associated with this article can be found in the online version.

Acknowledgments

We thank Latika Nagpal and Kaushik Bhar for their technical assistance.

Appendix A. Supplementary data

Supplementary data associated with this article can be found, in the online version, at http://dx.doi.org/10.1016/j.toxrep.2016.02.001.

References

[1] CDC, The Health Consequence of Smoking: A Report of the Surgeon General, US Department of Health and Human Services, Atlanta, GA, 2004.
[2] ACS, Prevention and Early Detection. Guide to Quitting Smoking, American Cancer Society, Atlanta, 2010 http://www.cancer.Org/Healthy/Stayawayfromtobacco/Guidetoquittingsmoking/I.
[3] USDHHS, 1989. Centers for Disease Control, Center for Chronic Disease Prevention and Health Promotion, Office on Smoking and Health Reducing the Health Consequence of Smoking: 25 Years of Progress. A Report of the Surgeon General; (1989). DHHS Publication (CDC) 89–8411 (1989).
[4] USDHHS. Centers for Disease Control and Prevention : The health consequence of smoking: a report of the Surgeon General. Atlanta, GA (2004).
[5] J.L. Fellows, A. Trosclair, National Center for Chronic Disease Prevention and Health Promotion, CDC, Annual Smoking-Attributable Mortality, Years of Potential Life Lost and Economic Costs-United States, 1995–1999., Morbidity and Mortality Weekly Report, 51, (2002), 300–303.
[6] J.A. Jensen, W.H. Goodson, H.W. Hopf, T.K. Hunt, Cigarette smoking decreases tissue oxygen, Arch. Surg. 126 (1991) (1991) 1131–1134.
[7] A. Afaqa, P.A. Montgomery, K. Scott, S.M. Blevins, T.L. Whitsetta, A.W. Gardnerb, The effect of current cigarette smoking on calf muscle hemoglobin oxygen saturation in patients with intermittent claudication, Vasc. Med. 12 (2007) 167–173.
[8] M.L. Socol, F.A. Manning, Y. Murata, M.L. Druzin, Maternal smoking causes fetal hypoxia, Am. J. Obstet. Gynecol. 142 (1990) 214–218.
[9] M.G. Bulterys, S. Greenland, J.F. Kraus, Chronic fetal hypoxia and sudden infant death syndrome: interaction between maternal smoking and low hematocrit during Pregnancy, Pediatrics 86 (1990) 535–540.
[10] USDHHS. Centers for Disease Control and Prevention : The health consequence of smoking: a report of the Surgeon General Atlanta, GA 2001.
[11] M. Prelog, Smoking and Reproduction, in Cigarette Smoke Toxicity: Linking Individual Chemicals to Human Diseases, in: D. Bernhard (Ed.), Wiley-VCH Verlag GmbH & CoKGaA, Weinheim, Austria, 2011, pp. 217–237.
[12] W.A. Pryor, K. Stone, L.-Y. Zang, E. Bermudez, Fractionation of aqueous cigarette tar extracts: fractions that contain the tar radical cause DNA damage, Chem. Res. Toxicol. 1 (1998) (1998) 441–448.
[13] S. Sen, C. Peltz, J. Beard, B. Zeno, Recurrent carbon monoxide poisoning from cigarette smoking, Am. J. Med. Sci. 340 (2010) 427–429.
[14] L.K. Weaver, S. Howe, R. Hopkins, K.J. Chan, Carboxyhemoglobin half-life in carbon monoxide-poisoned patients treated with 100% oxygen at atmospheric pressure, Chest 117 (2000) 801–808.
[15] I. B. Chatterjee, Process for the isolation of a major harmful oxidant from cigarette smoke. US Patent (2005) No. 6929012.
[16] N. Dey, A. Das, A. Ghosh, I.B. Chatterjee, Activated charcoal filter effectively reduces *p*-benzosemiquinone from the mainstream cigarette smoke and prevents emphysema, J. Biosci. 35 (2010) 217–230.
[17] S. Banerjee, R. Chattopadhyay, A. Ghosh, H. Koley, K. Panda, S. Roy, D. Chattopadhyay, I.B. Chatterjee, Cellular and molecular mechanisms of cigarette smoke-induced lung damage and prevention by vitamin C, J. Inflamm. (Lond.) 5 (2008) 21.
[18] A. Ghosh, A. Choudhury, A. Das, N.S. Chatterjee, T. Das, R. Chowdhury, K. Panda, R. Banerjee, I.B. Chatterjee, Cigarette smoke induces *p*-benzoquinone-albumin adduct in blood serum: implications on structure and ligand binding properties, Toxicology 292 (2012) 78–89.
[19] N. Dey, D.J. Chattopadhyay, I.B. Chatterjee, Molecular mechanisms of cigarette smoke induced proliferation of lung cells and prevention by vitamin C, J. Oncol. (2011), Article ID 561862.
[20] D. Voet, J.G. Voet, Biochemistry, 3rd ed., Wiley International ed., USA, 2004, pp. 340.
[21] R. Das, G. Mitra, B. Mathew, C. Ross, V. Bhat, A.K. Mandal, Automated analysis of hemoglobin variants using nano LC–MS and customized databases, J. Proteom. Res. 12 (2013) 3215–3222.
[22] Y.H. Chen, J.T. Yang, H.M. Martinez, Determination of the secondary structures of proteins by circular dichroism and optical rotatory dispersion, Biochemistry 11 (1972) 4120–4131.
[23] S. Chlopicki, R. Olszanecki, E. Marcinkiewicz, M. Lomnicka, R. Motterlini, Carbon monoxide released by CORM-3 inhibits human platelets by a mechanism independent of soluble guanylate cyclase, Cardiovasc. Res. 71 (2006) 393–401.
[24] E. Antonini, M. Brunori, Hemoglobin, Annu. Rev. Biochem. 39 (1970) 977–1042.
[25] H. Smith, E.B. Mann, R. Motterlini, R.K. Poole, The carbon monoxide-releasing molecule, CORM-3 (Ru(CO) 3Cl(glycinate)), targets respiration and oxidases in campylobacter jejuni, generating hydrogen peroxide, IUBMB Life 63 (5) (2011) 363–371.
[26] J. Kim, A.R. Vaughn, C. Cho, T.V. Albu, E.A. Carver, Modifications of ribonuclease A induced by *p*-benzoquinone, Bioorg. Chem. 40 (2012) 92–98.
[27] P. Yu, I. Strug, T.R. Cafarella, B.A. Seaton, A. Krantz, Site-specific crosslinking of annexin proteins by 1,4-benzoquinone: a novel crosslinker for the formation of protein dimers and diverse protein conjugates, Org. Biomol. Chem. 10 (2012) (2012) 4500–4504.
[28] R. Schneider, A. Mayer, W. Schmatz, J. Schelten, R. Franzel, H. Eicher, X-ray and neutron small-angle scattering from hemoglobin in aqueous solution and in crystal, Eur. J. Biochem. 20 (1971) 179–182.
[29] A.K. Mandal, M.R. Ramasamy, V. Sabareesh, M.E. Openshaw, K.S. Krishnan, P. Balaram, Sequencing of T-superfamily conotoxins from Conus virgo:

pyroglutamic acid identification and disulfide arrangement by MALDI mass spectrometry, J. Am. Soc. Mass Spectrom. 18 (2007) 1396–1404.
[30] X. Wang, B. Thomas, R. Sachdeva, L. Arterburn, L. Frye, P.G. Hatcher, D.G. Cornwell, J. Ma, Mechanism of arylating quinone toxicity involving Michael adduct formation and induction of endoplasmic reticulum stress, Proc. Natl. Acad. Sci. U. S. A. 103 (2006) 3604–3609.
[31] F.B. Pipkin, Genetics of preeclampsia consortium. Smoking in moderate/severe preeclampsia worsens pregnancy outcome, but smoking cessation limits the damage, Hypertension 51 (2008) 1042–1046.
[32] L. Townsend, R.L. Maynard, Effects on health of prolonged exposure to low concentrations of carbon monoxide, Occup. Environ. Med. 59 (2002) 708–711.